Carboxylic acid-functionalized clathrochelate complexes: large, robust and easy-to-access metalloligands

Mathieu Marmier,[a] Matthew D. Wise,[a] Julian J. Holstein,[b] Philip Pattison,[c,d] Kurt Schenk,[c] Euro Solari,[a] Rosario Scopelliti,[a] and Kay Severin*[a]

[a] Institut des Sciences et Ingénierie Chimiques, École Polytechnique Fédérale de Lausanne (EPFL), CH-1015 Lausanne, Switzerland

[b] GZG, Department of Crystallography, Georg-August-Universität Göttingen, 37077 Göttingen, Germany

[c] Laboratory of Crystallography, Ecole Polytechnique Fédérale de Lausanne (EPFL), 1015 Lausanne, Switzerland

[d] Swiss-Norwegian Beamline, ESRF, Grenoble, France

ABSTRACT: Polycarboxylate ligands are among the most important building blocks for the synthesis of metal-organic frameworks (MOFs). The ability to access these ligands in an efficient way is of key importance for future applications of MOFs. Here, we demonstrate that mono- and dinuclear clathrochelate complexes are versatile scaffolds for the preparation of polytopic carboxylate ligands. The largely inert clathrochelate complexes have a trigonal bipyramidal shape. The synthesis of functionalized clathrochelates with two, three, four or five carboxylic acid groups in the ligand periphery can be achieved in few steps from simple starting materials. Apart from being easily accessible, the metalloligands display interesting characteristics for applications in metallasupramolecular chemistry and materials science: they are rigid, large (up to 2.2 nm), robust, and they can show additional functions (e.g. fluorescence or extra charge) depending on the metal ion that is present in the clathrochelate core. The utility of these new metalloligands in MOF chemistry is demonstrated by the synthesis of Zn- and Zr-based coordination polymers. The combination of $Zn(NO_3)_2$ with clathrochelates having two or three carboxylic acid groups gives MOFs in which the clathrochelate ligands are connected by Zn_4O clusters or Zn paddlewheel links. The structures of the resulting two- and three-dimensional networks could be established by single crystal X-ray crystallography. The reaction of carboxylic acid-functionalized clathrochelates with $ZrCl_4$ gives amorphous powders which display permanent porosity after solvent removal.

INTRODUCTION

Carboxylic acid-functionalized ligands are of paramount importance in supramolecular chemistry, most notably in the preparation of metal–organic frameworks (MOFs). Since the pioneering discovery of compounds such as MOF-5 by Yaghi and coworkers,[1] and HKUST-1 by the group of Williams,[2] the number of reported MOF structures continues to grow exponentially.[3]

The development of MOF chemistry has in part been driven by the variety of ligands employed in the preparation of these materials. The concept of reticular chemistry,[4] along with a range of well-established synthetic techniques for MOF preparation, has enabled the strategic incorporation of increasingly elaborate ligands into MOFs, the properties and structural characteristics of which are determined by those of the ligands themselves. This powerful, modular means to prepare bespoke materials in a targeted manner is exemplified by MOF-5 and its isoreticular analogues, which have been constructed from a wide range of ditopic carboxylic acid ligands such as those based on extended oligo(phenylenes) and terephthalic acid derivatives,[5] and even metal complexes (metalloligands).[6] The incorporation of functional moieties, including photoactive groups,[7] catalytically active metal centers,[8] or simple organic functional groups,[9] into carboxylic acid-based MOF building blocks has facilitated the preparation of materials with new and interesting properties.

Another ligand property that has received a significant amount of attention in recent times is size. The preparation of longer or expanded building blocks has enabled MOFs with greater internal void volumes, cavity dimensions and surface areas to be made. Consequently, these materials are, for example, capable of the uptake of larger guest species[10] or greater volumes of adsorbed gas.[11] Again, reticular synthesis has encouraged the design of numerous expanded MOF structures based upon well-known network topologies,[12] but common setbacks encountered during research into these materials include the observation of extensive network interpenetration.[13] Other obstacles are the synthetic efforts and the costs associated with the preparation of large ligands. This point is exemplified by work of the groups of Yaghi and Stoddart,[14] who developed a series of ditopic linear α-hydroxycarboxylic acid ligands up to 5 nm in length. These building blocks were subsequently incorporated into a range of isostructural MOFs (the IRMOF-74 series), which possessed interior channel apertures of up to 98 Å. The synthesis of the longest ligand employed in this study required eight steps and gave an overall yield of 14%.

Herein, we report a means to efficiently prepare large di-, tri-, tetra- and pentatopic carboxylic acid ligands in few steps from simple starting materials. Our ligands consist of trigonal bipyramidal clathrochelate complexes to which carboxylic acid groups may be appended in a modular manner (Figure 1). To demonstrate the utility of these metalloligands[15,16] in structural supramolecular chemistry, we have prepared a series of new coordination polymers, in which the clathrochelates are linked by Zn-or Zr-clusters to give two- or three-dimensional networks.

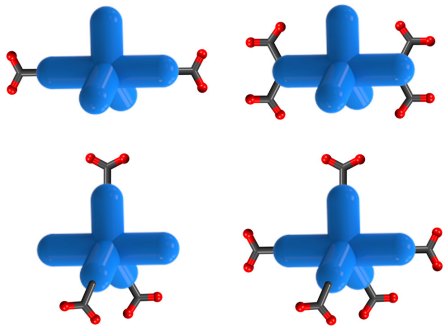

Figure 1. Schematic representation of the polycarboxylate ligands described herein. The carboxylic acid groups are attached to mono- or dinuclear clathrochelate complexes with a trigonal bipyramidal shape (in blue).

RESULTS AND DISCUSSION

SYNTHESIS OF THE CLATHROCHELATES

In 2006, the group of Chaudhuri reported the synthesis and the structural characterization of a dinuclear Mn^{II} clathrochelate complex with bridging phenolatodioximato ligands and capping methylboronate esters.[17] We recently showed that it is possible to construct 4,4'-bipyridyl ligands based on similar dinuclear complexes by replacing the terminal methylboronate esters with pyridylboronate esters.[18] A unique feature of these pyridyl-capped metalloligands is their negative charge, which may bestow supramolecular assemblies with extra stability.

We hypothesized that dinuclear clathrochelates could also be used as scaffolds for the preparation of new polycarboxylate ligands, which should represent highly interesting building blocks for MOF chemistry. Indeed, anionic M(II) tris(dioximato) complexes (M^{2+} = Co, Zn) with two appended carboxylic acid groups were obtained by reaction of 4-carboxyphenylboronic acid, 2,6-diformyl-4-*tert*-butylphenol dioxime (**L_1**) or 2,6-diformyl-4-bromophenol dioxime (**L_2**) and the appropriate metal salt ($Zn(OTf)_2$ or $[Co(H_2O)_6](NO_3)_2$) in a mixture of MeOH and EtOH (Scheme 1). It should be noted that the boronic acid is commercially available, and the dioximes can be prepared easily from the corresponding dialdehydes. Conversely to the synthesis of the pyridyl-capped clathrochelates reported previously,[18] presence of a base was required for the insertion of the third phenolatodioximato ligand. Tetraethylammonium hydroxide was chosen for this purpose since the NEt_4^+ cation enhances the solubility of the final complexes. The products **1**–**4** precipitated from solution upon concentration of the mother liquor as amorphous solids. The high yields of 74−92% indicate that the CO_2H functions on the boronic acid do not interfere with the formation of the dinuclear clathrochelate core, even though Zn^{2+} and Co^{2+} ions are known to bind carboxylate ligands. The anionic clathrochelates **1**–**4** are well soluble in polar aprotic solvents such as DMF, DMA and DMSO.

Scheme 1. Synthesis of the ditopic clathrochelate complexes 1–4.

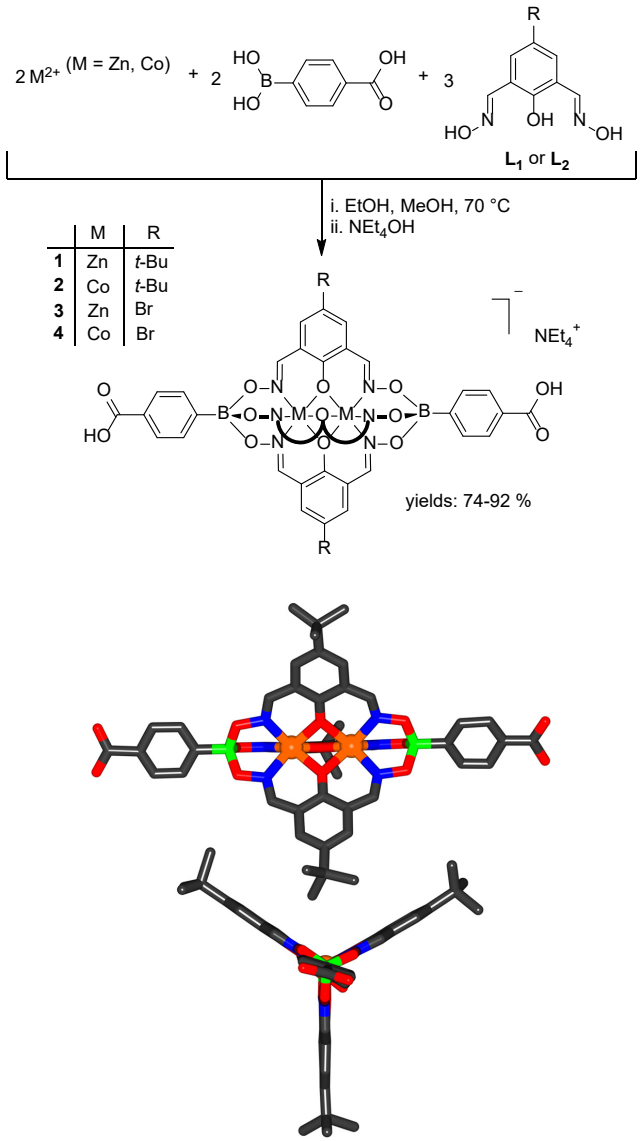

Figure 2. Molecular structure of metalloligand **2** in the crystal with view from the side (top) and along the pseudo-C_3 symmetry axis (bottom). Hydrogen atoms, the counter ion (NEt_4^+), and solvent molecules have been omitted for clarity. Color coding: C: gray; O: red; N: blue; B: green; Co: orange.

Clathrochelates **1**–**4** were analyzed by high-resolution mass spectrometry, Fourier-transform infrared spectroscopy and, for the diamagnetic complexes **1** and **3**, NMR spectroscopy. As expected, only one set of signals was observed for the phenolatodioximato ligands, revealing the *pseudo*-C_3 symmetry of the complexes. Single crystal X-ray structural analysis of **2** revealed the presence of the expected dinuclear clathrochelate core with terminal carboxylic acid groups (Figure 2).

The two Co^{2+} ions in complex **2** are coordinated in a trigonal prismatic fashion by three nitrogen and three oxygen atoms. The two carbon atoms of the terminal CO_2H groups are 21 Å apart from each other. This length is notably far from the 50Å of IRMOF-74-XI ligand,[14] but the synthetic efforts cannot be confronted. Clathrochelate **2** is however comparable to ditopic linkers having up to five phenylene spacers, such as ligand V (about 22Å) in the IRMOF-74-V,[14] or slightly larger than *trans*-biscarboxylate tetraarylporphyrins such as $H_4DCPMes_2P$ in

PIZA-4,[19] or ditopic ligands with four aryl rings spacers.[20] In solution, the Zn complexes **1** and **3** display pseudo-C_3 symmetry as revealed by a single set of NMR signals for the three oximato ligands. In the solid state, one can observe a small deviation from this 'ideal' geometry, with angles between the planes of the three lateral oximato ligands between 116.90° and 123.13° (Figure 2, bottom).

Scheme 2. Synthesis of the tetratopic clathrochelate complex 5.

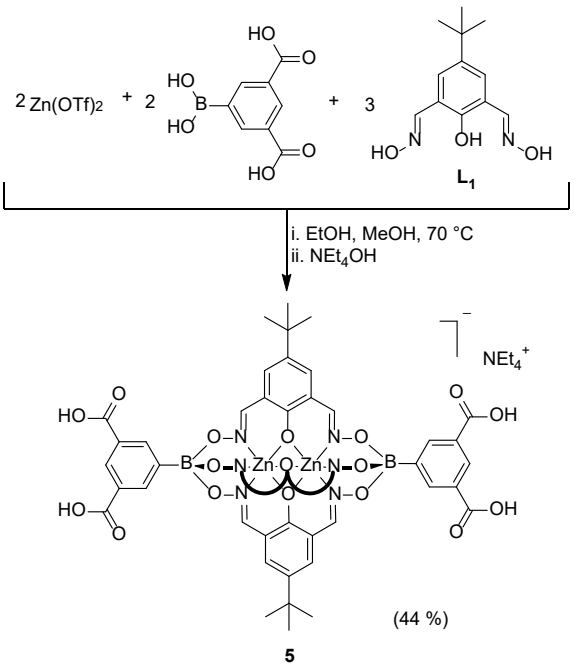

A similar synthetic strategy as employed for **1**–**4** was used to prepare the clathrochelate complex **5** featuring four carboxylic acid functions attached to the terminal arylboronate ester groups (Scheme 2). Clathrochelate **5** was obtained as a fully protonated tetraethylammonium salt in 44% yield, and characterized by high-resolution mass spectrometry, Fourier-transform infrared spectroscopy and NMR.

In addition to the anionic, dinuclear clathrochelates presented above, we have prepared mononuclear clathrochelate complexes with terminal CO_2H groups (**6**–**11**). The synthesis of these complexes was achieved by reaction of anhydrous $FeCl_2$ with commercial dioximes and 3- or 4-carboxyphenylboronic acid, respectively (Scheme 3). The ditopic complexes **6** and **8** are known,[21] but applications in supramolecular chemistry have not been reported. We have prepared the novel, less sterically bulky analogues **7** and **9** using dimethylglyoxime. A closely related approach was subsequently employed in the synthesis of the tetratopic clathrochelates **10** and **11**. All complexes were characterized by high-resolution mass spectrometry and NMR spectroscopy. In contrast to the ionic compounds **1**–**5**, the difunctional clathrochelates **6**–**9** are soluble in organic solvents such as dichloromethane, with the dimethylglyoxime-derived complexes **7** and **9** being slightly less soluble than the nioxime-derived complexes **6** and **8** (nioxime = 1,2-cyclohexanedione-dioxime). Tetratopic clathrochelates **10** and **11** are soluble in polar aprotic solvent, such as DMSO and DMF.

Scheme 3. Synthesis of the mononuclear clathrochelate complexes 6–11.

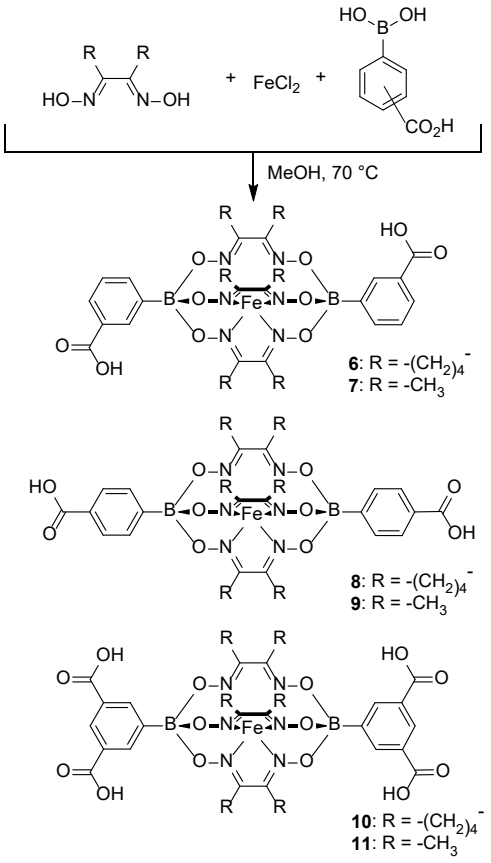

The structures of **6** and **8** were analyzed by single crystal X-ray diffraction (Figure 3). These crystal structures reveal the characteristic trigonal prismatic coordination geometry of the encapsulated low spin Fe(II) ion,[22] in which Fe–N distances vary from 1.908(3) to 1.916(3) in **6** and 1.904(5) to 1.931(3) in **8**. The two carbon atoms of the terminal CO_2H groups in complex **8** are 17.921(2) Å apart from each other.

The clathrochelate complexes **1**–**11** feature either two or four CO_2H groups, which were introduced during the synthesis by using a functionalized arylboronic acid. The oximato ligands occupy lateral positions with respect to the axis defined by the two boron atoms. By using different oximato ligands, we have demonstrated that it is possible to change the size and the solubility of the metalloligands independently from the function-defining boronic acid.

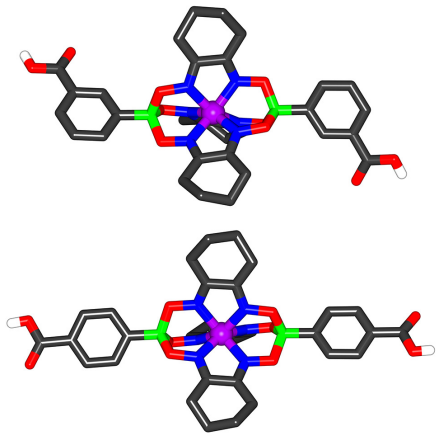

Figure 3. Molecular structures of the complexes **6** (top) and **8** (bottom) in the crystal. C–H hydrogen atoms and solvent molecules have been omitted for clarity. Color coding: C: gray; O: red; N: blue; B: green; Fe: purple.

We envisioned that it should also be possible to use the oximato ligands for introducing additional CO_2H groups, thereby broadening the variety and hence potential applications of clathrochelate-based metalloligands. This goal was accomplished through synthesis of the CO_2H-functionalized dioximato ligand **L3**. Suzuki-Miyaura coupling of 4-carboxyphenylboronic acid and 2,6-diformyl-4-bromophenol in the presence of $Pd_2(dba)_3$ and Buchwald's SPhos ligand[23] in *n*-BuOH afforded the crude diformylphenol intermediate, which was converted to its corresponding dioxime **L3** by treatment with hydroxylamine hydrochloride (Scheme 4).

Scheme 4. Synthesis of ligand L3.

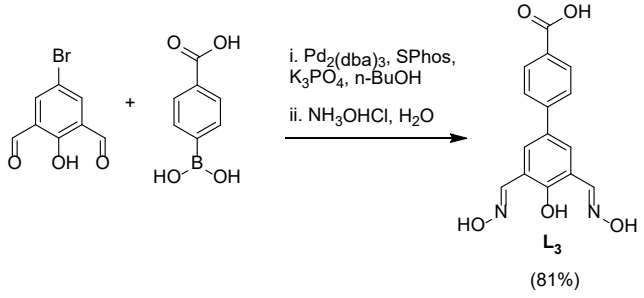

The new ligand **L3** was subsequently used for the synthesis of the clathrochelates **12** and **13** (Scheme 5). These complexes feature three CO_2H groups in equatorial position and two bromo atoms in axial position. Based on simple molecular modelling considerations, we expect a distance of approximately 18.6 Å between the carbon atoms of the carboxylic acid groups. Consequently, these trigonal metalloligands are significantly larger than the commonly employed 1,3,5-tris(4-carboxyphenyl)benzene ligand (C···C = 12.55 Å). The bromo atoms were introduced because they were found to slightly improve the solubility of the clathrochelates.

By using ligand **L3** in combination with the capping agent 4-carboxyphenylboronic acid, we obtained the pentatopic clathrochelate ligands **14** and **15** (Scheme 5). To date, very few examples of 5-fold coordinating ligands have been studied,[24] and our clathrochelates are, to the best of our knowledge, the largest such ligands ever reported.

Scheme 5. Synthesis of the tri- and pentatopic clathrochelate complexes 12–15.

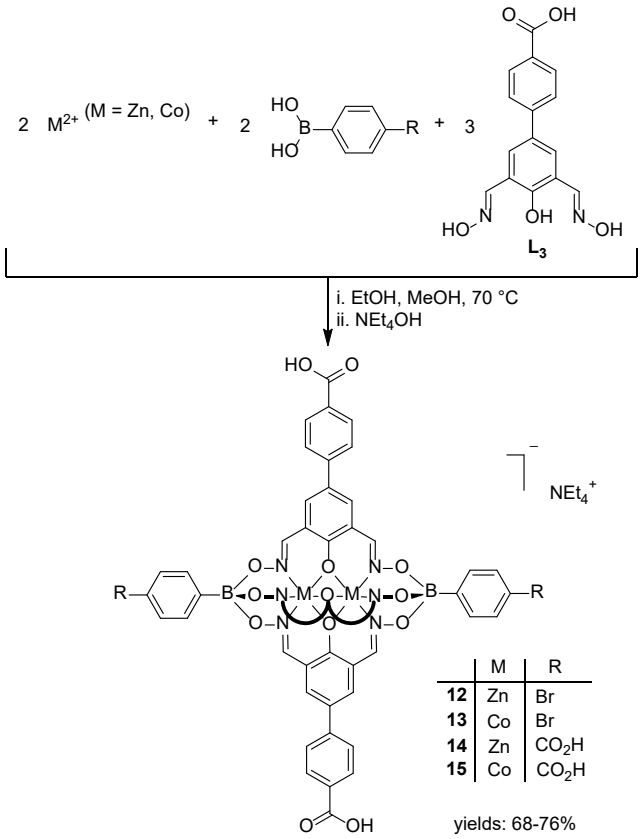

In the discussion so far, we have mainly focused on the size and the geometry of the new metalloligands. However, there are also other properties which are worth noting. The Zn-based clathrochelates **1**, **3**, **5**, **12**, and **14** are all luminescent, with emission maxima at around 450 nm (**1**: 445nm, λ_{ex} = 325nm; **3**: 452nm, λ_{ex} = 335nm; **5**: 445nm, λ_{ex} = 335nm; **12**: 457nm, λ_{ex} = 335nm; **14**: 445nm, λ_{ex} = 335nm, in DMF/DMSO, Figure S37 and S38). Due to the inert character of the Zn^{2+} ions, the luminescence can be assigned to intraligand and/or ligand-to-ligand charge transfer emissions. The dinuclear Co complexes are not emissive, presumably due to quenching by the paramagnetic metal ions. The magnetic properties of the Co clathrochelates were not studied in detail, however for complexes **2** and **4** we have determined effective magnetic moments (μ_{eff}) of 5.37 μ_B and 5.81 μ_B, respectively, by using the Evans method. We would also like to stress the intrinsic charge displayed by the dinuclear Zn and Co-containing clathrochelates. This additional negative charge represents a fundamental difference compared to standard carboxylic acid ligands, which only become charged after deprotonation of the CO_2H groups.

UTILIZATION AS METALLOLIGANDS IN MOFs

Having shown that carboxylic acid-functionalized clathrochelate complexes can be synthesized in one pot from simple and readily available starting materials, we examined applications as supramolecular building blocks. Based on their structures, it was not established that the clathrochelate core would survive the relative harsh conditions employed for MOFs syntheses. The lateral side groups of the oximes were also a challenging part, since it was difficult to estimate if the steric bulk from adjacent clathrochelates was not a pitfall for the formation of rectangular coordination pattern found in many MOFs. On the other hand, the lateral groups could be found as a virtue,

preventing interpenetration of the networks. The effect of the intrinsic negative charge shared by the bimetallic clathrochelates was also an unknown parameter to take into account.

In order to demonstrate that our clathrochelate-based polycarboxylic acids are suitable for incorporation into MOFs, we targeted the syntheses of two representative coordination polymer classes, the first one sharing MOF-5 topology, the second one related to zirconium-based MOFs. MOF-5 is amongst the most extensively studied porous materials since its discovery in 1999,[1] and given the vast rage of isostructural MOF-5 analogues that have been reported, along with the interesting functional properties possessed by many of these materials,[25] this framework structure was considered to be an ideal initial candidate for the incorporation of carboxylic acid-functionalized clathrochelate complexes into MOFs. Solvothermal reaction of ditopic ligands **1, 2** and **4** and $[Zn(H_2O)_6](NO_3)_2$ in a mixture of DMF and a chlorinated aromatic solvent (chlorobenzene, 1,2-dichlorobenzene or 1,2,4-trichlorobenzene) or DEF at 120°C resulted in the formation of single crystals upon heating (Scheme 6).

Scheme 6. Syntheses of the MOFs 16–20.

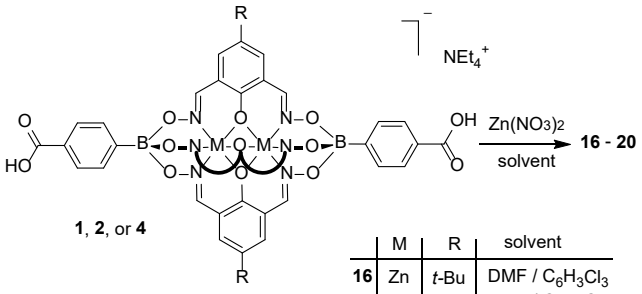

	M	R	solvent
16	Zn	*t*-Bu	DMF / $C_6H_3Cl_3$
17	Zn	*t*-Bu	DMF / $C_6H_4Cl_2$
18	Co	*t*-Bu	DMF / $C_6H_4Cl_2$
19	Co	*t*-Bu	DMF / $C_6H_3Cl_3$
20	Co	Br	DMF / DEF

Single crystals suitable for X-ray structural analysis were obtained for all the different solvent systems. Due to weak diffraction and the high disorder observed in the crystals, the key to a successful refinement was the utilization of stereochemical restraints for the clathrochelate ligands within MOFs **16**-**20**, which were generated by the GRADE program.[26,27] This macromolecular refinement technique has been adapted to be used in the program SHELXL.[28] We have already used this methodology for other clathrochelate-based structures,[16] and it was found to drastically increases the robustness of the refinement, especially when being combined with the new rigid bond restraint in SHELXL (RIGU).[29] The program ShelXle,[30] which supports the macromolecular residue grouping, was used as a GUI. The DSR program was employed to semi-automatically model disordered moieties.[31]

Crystallographic analysis of MOF **16** revealed a topology identical to MOF-5 and the IRMOF-n series.[32] The framework is composed of clathrochelate complexes ligated to Zn_4O clusters by their carboxylate groups (Figure 4). These clusters are composed of four tetrahedral Zn^{2+} cations and a central μ_4-O atom.

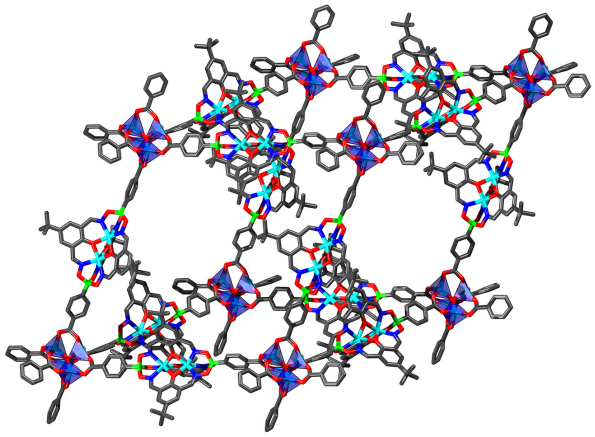

Figure 4. Part of the structure of MOF **16**. Hydrogen atoms, NEt_4^+ cations, and solvent molecules have been omitted for clarity. Color coding: C: gray; O: red; N: blue; B: green; Zn: cyan. Blue polyhedral represent the tetrahedral Zn atoms in the tetranuclear SBU.

Unlike MOF-5, where each Zn_4O node adopts an octahedral geometry with respect to the organic linkers, **16** showed a slightly distorted geometry. Indeed, the zinc SBUs are linked together by the deprotonated dicarboxylic acid ligands in a trigonal antiprismatic fashion. The central oxygen atoms from adjacent zinc SBUs are separated by a distance of 27.750(5) Å, the angles between the axis of the clathrochelate ligands (as defined by the central μ_4-O atoms of the Zn_4O nodes) are 71° and 109° for *cis*- pairs of clathrochelates, respectively, to be compared to the average 90° angle in the IRMOF-n series. Somewhat surprisingly, the network is two-fold interpenetrated (Figure S46). Such interpenetration has frequently been observed for MOF-5 assemblies constructed from long carboxylate ligands,[33] but we had anticipated that the steric bulk of the equatorial *tert*-butyl groups of the phenolatodioximato ligands within **1** might prevent such interpenetration. A unique feature of **16** compared to standard MOF-5-type structures is the fact that the network is negatively charged (the bridging carboxylate ligands display a charge of –3). The charge is compensated by NEt_4^+ cations, which are found in the voids of the structure.

Whereas structural analyses of MOFs **18** and **19** exhibited only minor structural differences compared to **16** (Figures S48–S51), presumably due to the different solvents employed during their synthesis, MOF **17** revealed different behavior. The three-dimensional framework is likewise composed of clathrochelate metalloligands connected to Zn_4O clusters (Figure 5). However, three of the Zn^{2+} cations adopt a classical tetrahedral geometry, whilst the fourth is six-coordinate and octahedral.

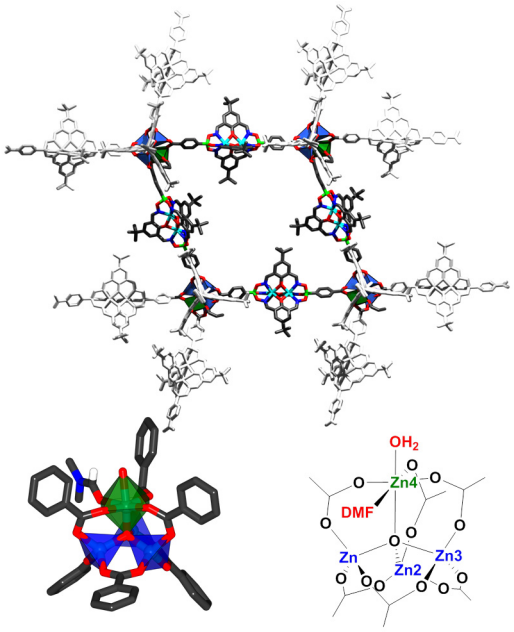

Figure 5. Part of the structure of MOF **17** with view along the crystallographic *c* axis (top) and molecular structure of the tetranuclear SBU (bottom). Most hydrogen atoms, NEt_4^+ cations, and solvent molecules have been omitted for clarity. Color coding: C: gray; H; white; O: red; N: blue; B: green; Zn: cyan. Blue and green polyhedra represent the tetrahedral and octahedral Zn atoms in the tetranuclear SBU, respectively.

Several groups have studied the exchange of one tetrahedral Zn^{2+} ion within a Zn_4O SBU with another, octahedral metal ion,[34] but reports of the formation of unusual geometries for one of the Zn^{2+} ions are scarce. Notably, the group of Gao reported in 2010 the synthesis of a rare Kagomé topology with a five-coordinate trigonal bipyramidal geometry for one of the Zn^{2+} ions and an octahedral geometry for another after binding of two DMSO molecules.[35] Within the Zn_4O clusters of **17**, three Zn^{2+} ions (Zn1, Zn2 and Zn3) are located in tetrahedral environments, each metal ion being coordinated by three carboxylate oxygen atoms from different clathrochelate ligands and the μ_4-O atom in the center of the cluster (Figure 5, bottom). The remaining zinc atom (Zn4) adopts an unusual octahedral geometry, coordinated by the μ_4-O central atom, three carboxylate oxygen atoms and two extra oxygen atoms that were attributed to one DMF molecule and one water molecule, the latter coming most likely from the hydrated zinc salt used in the synthesis of the MOFs. It should be noted that the unusual SBU can be found in the bulk material of **17** as evidenced by powder XRD, but due to the poor quality of the diffraction data, we cannot exclude the presence of small amounts of a different phase (Figure S56).

The presence of one octahedral Zn^{2+} ion within the Zn_4O cluster significantly affects the structure of MOF **17**. In contrast to the IRMOF-n series or MOF **16**, where the tetranuclear cluster connects three collinear pairs of bis(carboxylate) ligands, MOF **17** contains one pair of clathrochelate ligands, the axis of which are tilted with respect to each other. The angles between opposite pairs of clathrochelate ligands are 180°, 180° and 135°. The latter results in a distortion of the framework structure, which displays a zigzag shape along the crystallographic *c* axis (Figure 5, top). The central μ_4-O atoms of adjacent Zn_4O SBUs are separated by a distance of 27.471(2) Å and 27.894(1) Å, the latter being only slightly longer than for **16**. The coordination of one DMF molecule to one of the Zn^{2+} ions in the tetranuclear cluster was only observed for MOF **17**, whereas **16, 18**, and **19** did not feature this asymmetric SBU. A convincing rationale for the formation of this octahedral Zn^{2+} ion has not yet been formulated.

We also investigated the formation of network structures using metalloligand **4** having less sterically demanding phenolatodioximato ligands (Br instead of *tert*-butyl*)*. Solvothermal treatment of **4** with $Zn(NO_3)_2(H_2O)_6$ in a DMF/DEF mixture at 120°C resulted in the formation of orange cubic single crystals of MOF **20** (Scheme 6). Structural analysis of **20** revealed minor differences compared to **17–19** (Figure S52 and S53). Reducing considerably the steric bulk by exchanging the *tert*-butyl side chains by a bromo substituent did not influence the network interpenetration (2-fold). The channels found in **20** are occupied by the NEt_4^+ cations, however the global disorder of the crystal did not allow us to locate precisely its alkyl chains.

In order to assess the gas sorption properties of the Zn-based MOFs **17–20**, nitrogen physisorption experiments were performed. BET surface measurements (N_2, 77K) after activation of the crystals by heating at 150°C under dynamic vacuum gave only low values (**16**: 98 m^2/g; **17**: 125 m^2/g; **18**: 58 m^2/g; **19**: 26 m^2/g; **20**: 32 m^2/g). The low N_2 adsorption is likely due to the two-fold interpenetration of the networks and due to the presence of the NEt_4^+ cations, resulting in a drastically reduced accessible void volume. Digestion ^{1}H-NMR of **16-20** after the gas sorption measurement revealed the presence of residual DMF despite the activation process (Figures S27–S31). Digestion ^{1}H-NMR experiments also unambiguously confirmed the presence of the NEt_4^+ cations within the network pores. Attempts to activate the crystals by solvent exchange with methanol or acetone gave even lower values for the BET measurements due to the collapse of networks during the exchange process. The sensitivity of the network structure was confirmed by powder XRD analyses of **16** and **18–20**, which revealed complete loss of crystallinity upon drying of the materials.

Having shown that bimetallic clathrochelates can be incorporated in MOF structures, we attempted similar syntheses using the iron(II) tris(dioxime) clathrochelate **8**. However, in combination with $[Zn(H_2O)_6](NO_3)_2$ in DMA, we observed the formation of the 2D-layered coordination polymer **21** (Scheme 7). The coordination polymer **21** is comprised of 2D sheets, in which doubly deprotonated molecules of **8** bridge between Zn^{2+} paddlewheel SBUs (Figure 6).[36] DMA molecules are coordinated to the apical positions of the Zn^{2+} ions. Each layer of **21** is identical in its composition and orientation, but rather than eclipsing one another when viewed perpendicular to the plane of a single Zn(**8**) sheet, the layers are offset by 7.76 Å. This structural feature is likely due to the steric clash of not only apical DMA molecules bound to Zn, but also the bulky cyclohexyl substituents of the clathrochelate complexes themselves. Despite the offset packing within **21**, 1D channels, filled with disordered solvent molecules in the crystal, permeate the material. The aperture and volume of these channels are determined by the steric bulk of the cyclohexyl groups of the clathrochelate oxime substituents. Removal of the guest solvent molecules led to a total collapsing of the coordination network structure, resulting in a non-porous material.

Scheme 7. Synthesis of MOF 21.

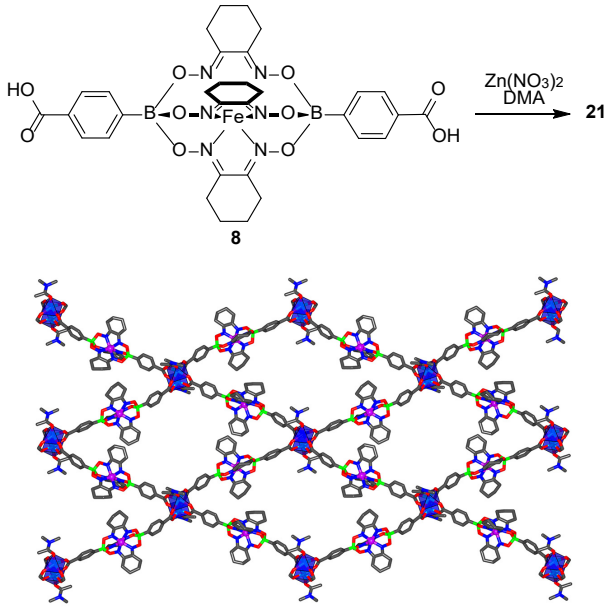

Figure 6. Part of the structure of MOF **21**. Hydrogen atoms and the non-bound solvent molecules have been omitted for clarity. Color coding: C: gray; O: red; N: blue; B: green; Zn: cyan; Fe: purple.

We also studied the formation of networks using our tritopic clathrochelate **12**. Reaction of **12** with $[Zn(H_2O)_6](NO_3)_2$ in a mixture of DMF and DMSO resulted in the formation of transparent block-shaped crystals of **22** (Scheme 8). Crystallographic analysis of **22** showed a three-dimensional network in which all carboxylic acid units of **12** are coordinated to a Zn_4O cluster (Figure 7). As it was observed for **17**, the zinc cluster is composed of three tetrahedral and one octahedral Zn^{2+} ion (shown as blue and green polyhedra respectively). The octahedral ion is coordinated by the central μ_4-O atom, three oxygen atoms from the deprotonated carboxylate groups, and two DMSO molecules. Several examples of tritopic carboxylate ligands connected by Zn_4O clusters have been reported so far, but to the best of our knowledge the presence of one octahedral zinc within the Zn_4O cluster is unprecedented.[37] Consequently, **22** displays a connectivity slightly different from what has been observed for MOFs constructed from tritopic carboxylates ligands. The network of **22** is two-fold interpenetrated and anionic, hence contains NEt_4^+ cations as verified by digestion NMR (Figure S32), leading to a material with very low porosity (BET surface area of 21 m^2/g).

Scheme 8. Synthesis of MOF 22.

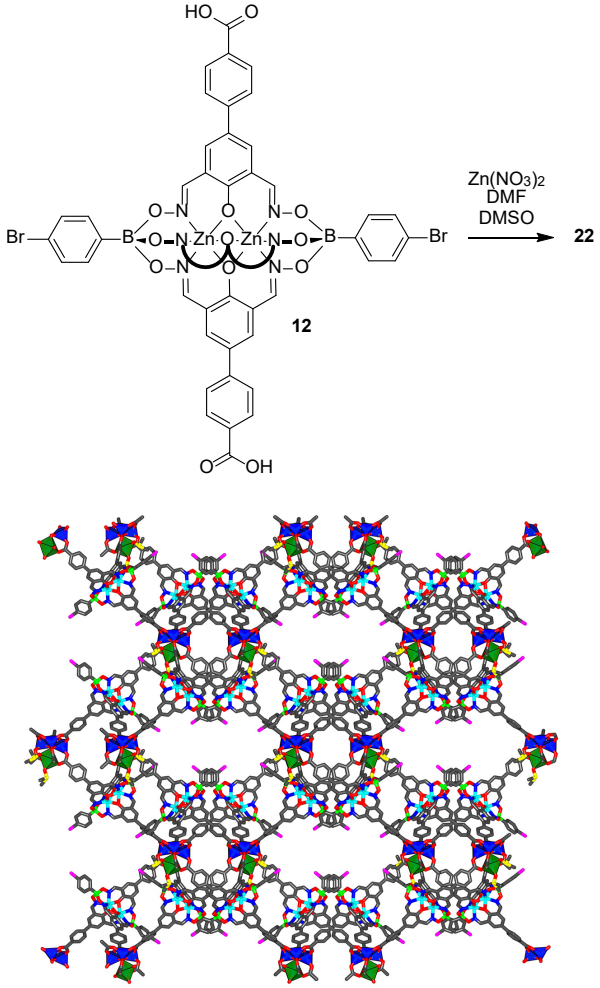

Figure 7. Part of the structure of MOF **22**. Hydrogen atoms, NEt_4^+ cations, and solvent molecules have been omitted for clarity. Color coding: C: gray; O: red; N: blue; B: green; Br: pink; S: yellow; Zn: cyan. Blue and green polyhedra represent the tetrahedral and respectively octahedral zinc atoms in the tetranuclear SBU.

In order to assess the versatility of our clathrochelates in the synthesis of other types of MOF, we turned to zirconium-based MOFs. In 2008, Lillerud and co-workers reported the synthesis of a new inorganic building unit, namely $Zr_6O_4(OH)_4(CO_2)_{12}$.[38] The solvothermal reaction between $ZrCl_4$ and terephthalic acic or terphenyldicarboxylic acid resulted in the formation of porous materials with specific surface areas of 1187 m^2g^{-1} and 4170 m^2g^{-1}, which were designated UiO-66 and UiO-68, respectively. Subsequent work has shown that the 12-fold coordinated cluster $Zr_6O_4(OH)_4(CO_2)_{12}$ can be reduced to 8-fold[39] and even 6-fold SBUs[40] by using appropriate polycarboxylate ligands. MOFs based on Zr clusters have attracted a lot of attention because these materials can display very high chemical stability.[41] Capitalizing on this characteristic, numerous applications have emerged over the last years, including the utilization of transition metal-functionalized Zr-MOFs as catalysts for organic syntheses,[42] or the utilization of Zr-MOFs for the hydrolytic decontamination of chemical warfare agents.[43]

Scheme 9. Synthesis of the Zr-MOFs 23–26.

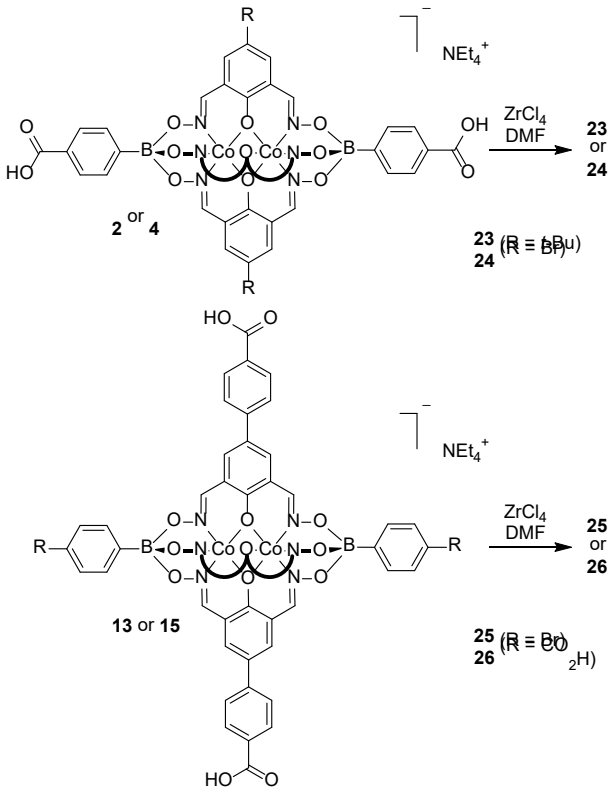

In order to examine if our clathrochelate-based metalloligands could be used to synthesize Zr-MOFs, we have investigated the reaction of the ditopic complexes **2** and **4** with $ZrCl_4$ in DMF. Initial worries that the clathrochelates would not withstand the rather harsh reaction conditions (120 °C, presence of the strong Lewis acid $ZrCl_4$) were not justified: after 3 days, we were able to obtain the Zr-MOFs **23** and **24** in the form of orange powders in good yields (Scheme 9).

Powder XRD analyses of **23** and **24** showed that the materials were poorly (**24**, Figure S57) or non-crystalline (**23**). Attempts to increase the crystallinity by using modulators such as benzoic or acetic acid[44] were unfortunately, not successful. In view of the poorly resolved PXRD spectra, we can only speculate about the type of Zr cluster which is present in **23** and **24**. Based on steric considerations, even the 12-fold coordinated Zr_6 cluster seems possible despite the substantial lateral size of metalloligand **2** (Figure S55). Interestingly, **23** and **24** appear to be neutral network structures because the NMR spectra of digested samples do not show signals corresponding to the NEt_4^+ cations (Figure S33 and S34). The necessary charge compensation could be accomplished by exchange of a hydroxide for a water ligand on the Zr cluster.

Encouraged by the successful synthesis of **23** and **24**, we have subsequently investigated the utilization of the tri- and the pentatopic metalloligands **13** and **15**. The observations were similar as before: after 3 days (DMF, 120 °C), we were able to collect orange, amorphous powders (**25** and **26**, Scheme 9). The absence of NEt_4^+ cations in **25** and **26** was again confirmed by digestion experiments.

In contrast to the Zn-based MOFs **16**–**22**, the Zr-based MOFs were all found to display substantial permanent porosity after removal of the solvent by heating at 150°C under dynamic vacuum. BET (N_2, 77K) measurements revealed specific surface areas of 410 m^2g^{-1} (**23**), 955 m^2g^{-1} (**24**), 535 m^2g^{-1} (**25**), and 546 m^2g^{-1} (**26**). It is worth noting that the surface area of **24** is more than twice of that of **23**. Both, **23** and **24**, are based on the same type of ditopic metalloligand, differing only in terms of the equatorial group R (Br vs. tert-butyl). This result suggests that it is possible to use the lateral oximato ligands for modulating the porosity of the MOFs. CO_2 (273K) physisorption experiments revealed high capacities for all Zr-MOFs, with MOF **24** being able to take up 85 cm^3g^{-1} at 1 bar. This value is slightly higher than what has been observed for UiO-66 derivatives.[45]

CONCLUSION

Mono- and dinuclear clathrochelate complexes with up to five pendent carboxylic acid groups have been be synthesized by metal-templated reactions using easily accessible starting materials. These rigid and robust complexes represent interesting metalloligands for applications in metallasupramolecular chemistry and materials science. The carboxylic acid functions are oriented in a divergent fashion, with well-defined coordinate vectors. In terms of size, the clathrochelates are comparable to carboxylic acid-functionalized porphyrin ligands, which have found numerous applications in the past.[46] A unique feature of our new metalloligands is their trigonal bipyramidal geometry. Such geometry is difficult to access with purely organic scaffolds.

To demonstrate the utility of carboxylic acid-functionalized clathrochelates in MOF chemistry, we have synthesized 2- and 3-dimensional network structures with zinc or zirconium clusters as SBUs. These preliminary results show that the metalloligands are compatible with reactions conditions employed for MOF synthesis, and that the steric bulk of the clathrochelates is not detrimental to the coordination of multiple metalloligands to one SBU. One should also note that the thermal and chemical stability of the clathrochelates is sufficient for many potential applications.

ASSOCIATED CONTENT

Experimental details, analytical data, crystallographic data, thermogravimetric analyses, N_2 and CO_2 physisorption measurements, and PXRD spectra. This material is available free of charge via the Internet at http://pubs.acs.org. Crystallographic data for the structures reported in this paper have been deposited at the Cambridge Crystallographic Data Center (CCDC) as supplementary publication no. CCDC 1441272 (**2**), 1439992 (**6**), 1439993 (**8**), 1439994 (**16**), 1439995 (**17**), 1439996 (**18**), 1439997 (**20**), 1439998 (**19**), 1439999 (**21**) and 1440000 (**22**). These data can be obtained free of charge from the Cambridge Crystallographic Data Centre via www.ccdc.cam.ac.uk/data_request/cif.

AUTHOR INFORMATION

Corresponding Author

* kay.severin@epfl.ch

Notes

The authors declare no competing financial interest.

ACKNOWLEDGMENT

The research leading to these results has received funding from the People Programme (Marie Curie Actions) of the European Union's Seventh Framework Programme FP7/2007-2013/ under REA grant agreement no 264645 (MDW and JJH), from the Swiss National Science Foundation, and from the EPFL. We are grateful to the

Swiss-Norwegian Beamline Consortium for providing access to synchrotron radiation.

REFERENCES

(1) Li, H.; Eddaoudi, M.; O'Keeffe, M.; Yaghi, O. M. *Nature* **1999**, *402*, 276–279.
(2) Chui, S. S.; Lo, S. M.-F.; Charmant, J. P. H.; Orpen, A. G.; Williams, I. D. *Science,* **1999**, *283*, 1148–1150.
(3) Zhou, H.-C.; Kitagawa, S. *Chem. Soc. Rev.* **2014**, *43*, 5415-5418.
(4) Selected examples: (a) Furukawa, H.; Cordova, K. E.; Keeffe, M. O.; Yaghi, O. M. *Science* **2013**, *341*; (b) Ockwig, N. W.; Delgado-Friedrichs, O.; O'Keeffe, M.; Yaghi, O. M. *Acc. Chem. Res.* **2005**, *38*, 176–82; (c) Yaghi, O. M.; O'Keeffe, M.; Ockwig, N. W.; Chae, H. K.; Eddaoudi, M.; Kim, J. *Nature,* **2003**, *423*, 705.
(5) Selected examples: (a) Lu, W.; Wei, Z.; Gu, Z.-Y.; Liu, T.-F.; Park, J.; Park, J.; Tian, J.; Zhang, M.; Zhang, Q.; Gentle, T.; Bosch, M.; Zhou, H.-C. *Chem. Soc. Rev.* **2014**, *43*, 5561-5593; (b) Cook, T. R.; Zheng, Y.; Stang, P. J. *Chem. Rev.* **2012,** *113*, 734-777; (c) Deng, H.; Doonan, C. J.; Furukawa, H.; Ferreira, R. B.; Towne, J.; Knobler, C. B.; Wang, B.; Yaghi, *Science* **2010,** *327*, 846–850; (d) Li, Q.; Zhang, W.; Miljanic, O. Š.; Sue, C.-H.; Zhao, Y.-L.; Liu, L.; Knobler, C. B.; Stoddart, J. F.; Yaghi, O. M., *Science* **2009,** *325*, 855–859; (e) Britt, D.; Tranchemontagne, D.; Yaghi, O. M., *Proc. Natl. Acad. Sci. U. S. A.* **2008,** *105*, 11623–11627; (f) Wong-Foy, A. G.; Matzger, A. J.; Yaghi, O. M. *J. Am. Chem. Soc.* **2006**, *128*, 3494-3495; (g) Eddaoudi, M.; Kim, J.; Rosi, N.; Vodak, D.; Wachter, J.; O'Keeffe, M.; Yaghi, O. M. *Science* **2002**, *295*, 469–472.
(6) Selected examples: (a) Kumar, G.; Gupta, R., *Chem. Soc. Rev.* **2013,** *42*, 9403–53; (b) Thanasekaran, P.; Luo, T.; Wu, J.; Lu, K. *Dalt. Trans.* **2012**, *41*, 5437–5453; (c) Chen, B.; Das, M. C.; Xiang, S.; Zhang, Z.; Chen, B. *Angew. Chem. Int. Ed.* **2011**, *2*, 10510–10520; (d) Xiang, S.-C.; Zhang, Z.; Zhao, C.-G.; Hong, K.; Zhao, X.; Ding, D.-R.; Xie, M.-H.; Wu, C.-D.; Das, M. C.; Gill, R.; Thomas, K. M.; Chen, B. *Nat. Commun.* **2011**, *2*, 204; (e) Song, F.; Wang, C.; Falkowski, J. M.; Ma, L.; Lin, W. *J. Am. Chem. Soc.* **2010**, *132*, 15390–15398.
(7) Selected examples: (a) Dong, Y.-B.; Li, Y.-A.; Zhao, C.-W.; Zhu, N.-X.; Liu, Q.-K.; Chen, G.; Liu, J.-B.; Zhao, X.-D.; Ma, J.-P.; Zhang, S. *Chem. Commun.* **2015**, Advance Article, DOI: 10.1039/c5cc07783d. (b) Lee, Y.; Kim, S.; Kang, J. K.; Cohen, S. M. *Chem. Commun.* **2015**, *51*, 5735–5738; (c) Zhang, Z.-M.; Zhang, T.; Wang, C.; Lin, Z.; Long, L.-S.; Lin, W. *J. Am. Chem. Soc.* **2015**, *137*, 3197-3200; (d) Zhang, T.; Lin, W. *Chem. Soc. Rev.* **2014**, *43*, 5982–5993; (e) Wang, C.; Xie, Z.; deKrafft, K. E.; Lin, W. *J. Am. Chem. Soc.* **2011**, *133*, 13445–13454.
(8) Selected examples: (a) Bhunia, A.; Dey, S.; Moreno, J. M.; Diaz, U.; Concepcion, P.; Van Hecke, K.; Janiak, C.; Van Der Voort, P. *Chem. Commun.* **2016**, DOI: 10.1039/C5CC09459C (b) Mondloch, J. E.; Katz, M. J.; Isley, W. C.; Ghosh, P.; Liao, P.; Bury, W.; Wagner, G. W.; Hall, M. G.; DeCoste, J. B.; Peterson, G. W.; Snurr, R. Q.; Cramer, C. J.; Hupp, J. T.; Farha, O. K. *Nat. Mater.* **2015**, *14*, 512–516; (c) Beyzavi, M. H.; Klet, R. C.; Tussupbayev, S.; Borycz, J.; Vermeulen, N. A.; Cramer, C. J.; Stoddart, J. F.; Hupp, J. T.; Farha, O. K. *J. Am. Chem. Soc.* **2014**, *136*, 15861–15864; (d) Liu, J.; Chen, L.; Cui, H.; Zhang, J.; Zhang, L.; Su, C.-Y. *Chem. Soc. Rev.* **2014**, *43*, 6011–6061; (e) Dhakshinamoorthy, A.; Alvaro, M.; Garcia, H. *Chem. Commun.* **2012**, *48*, 11275–11288; (f) Wang, C.; Wang, J.-L.; Lin, W. *J. Am. Chem. Soc.* **2012**, *134*, 19895–19908.
(9) Selected examples: (a) Furukawa, H.; Müller, U.; Yaghi, O. M. *Angew. Chem. Int. Ed.* **2015**, *54*, 3417–3430; (b) Henke, S.; Schneemann, A.; Fischer, R. A. *Adv. Funct. Mater.* **2013**, *23*, 5990–5996; (c) Park, J.; Yuan, D.; Pham, K. T.; Li, J.-R.; Yakovenko, A.; Zhou, H.-C. *J. Am. Chem. Soc.* **2012**, *134*, 99–102; (d) Henke, S.; Schneemann, A.; Wütscher, A.; Fischer, R. A. *J. Am. Chem. Soc.* **2012**, *134*, 9464–9474.
(10) Selected examples: (a) Li, P.-Z.; Wang, X.-J.; Tan, S. Y.; Ang, C. Y.; Chen, H.; Liu, J.; Zou, R.; Zhao, Y. *Angew. Chem. Int. Ed.* **2015**, *54*, 12748–12752. (b) Schneemann, A.; Bon, V.; Schwedler, I.; Senkovska, I.; Kaskel, S.; Fischer, R. A. *Chem. Soc. Rev.* **2014**, *43*, 6062–6096; (c) Qin, J.-S.; Zhang, S.-R.; Du, D.-Y.; Shen, P.; Bao, S.-J.; Lan, Y.-Q.; Su, Z.-M. *Chem. A Eur. J.* **2014**, *20*, 5625–5630.
(11) Selected examples: (a) Senkovska, I.; Kaskel, S. *Chem. Commun.* **2014**, *50*, 7089–7098; (b) Zhang, M.; Bosch, M.; Gentle, T.; Zhou, H. *CrystEngComm,* **2014**, *16*, 4069–4083; (c) Chaemchuen, S.; Kabir, N. A.; Zhou, K.; Verpoort, F. *Chem. Soc. Rev.* **2013**, *42*, 9304–9332; (d) Sumida, K.; Rogow, D. L.; Mason, J. A.; McDonald, T. M.; Bloch, E. D.; Herm, Z. R.; Bae, T.-H.; Long, J. R. *Chem. Rev.* **2012**, *112*, 724–781; (e) Farha, O. K.; Eryazici, I.; Jeong, N. C.; Hauser, B. G.; Wilmer, C. E.; Sarjeant, A. A.; Snurr, R. Q.; Nguyen, S. T.; Yazaydın, A. Ö.; Hupp, J. T. *J. Am. Chem. Soc.* **2012**, *134*, 15016–15021.
(12) Selected examples: (a) Guillerm, V.; Kim, D.; Eubank, J. F.; Luebke, R.; Liu, X.; Adil, K.; Lah, M. S.; Eddaoudi, M. *Chem. Soc. Rev.* **2014**, *43*, 6141–6172; (b) Li, M.; Li, D.; O'Keeffe, M.; Yaghi, O. M. *Chem. Rev.* **2013**, *114*, 1343–1370; (c) O'Keeffe, M.; Yaghi, O. M. *Chem. Rev.* **2012**, *112*, 675–702.
(13) Selected examples: (a) Jiang, H.-L.; Makal, T. A.; Zhou, H.-C. *Coord. Chem. Rev.* **2013**, *257*, 2232–2249; (b) Rankine, D.; Avellaneda, A.; Hill, M. R.; Doonan, C. J.; Sumby, C. J. *Chem. Commun.* **2012**, *48*, 10328–10330; (c) Mulfort, K. L.; Farha, O. K.; Malliakas, C. D.; Kanatzidis, M. G.; Hupp, J. T. *Chem. Eur. J.* **2010**, *16*, 276–281.
(14) (a) Deng, H.; Grunder, S.; Cordova, K. E.; Valente, C.; Furukawa, H.; Hmadeh, M.; Gándara, F.; Whalley, A. C.; Liu, Z.; Asahina, S.; Kazumori, H.; O'Keeffe, M.; Terasaki, O.; Stoddart, J. F.; Yaghi, O. M. *Science,* **2012**, *336*, 1018–1023; (b) Grunder, S.; Valente, C.; Whalley, A. C.; Sampath, S.; Portmann, J.; Botros, Y. Y.; Stoddart, J. F. *Chem. Eur. J.* **2012**, *18*, 15632–49.
(15) For reviews on metalloligands see: (a) Li, L.; Fanna, D. J.; Shepherd, N. D.; Lindoy, L. F.; Li, F. *J. Incl. Phenom. Macrocycl. Chem.* **2015**, *82*, 3−12; (b) Han, Y.-F.; Jin, G.-X. *Acc. Chem. Res.* **2014**, *47*, 3571–3579; (c) Kumar, G.; Gupta, R. *Chem. Soc. Rev.* **2013**, *42*, 9403–53; (d) Chen, B.; Das, M. C.; Xiang, S.; Zhang, Z.; Chen, B. *Angew. Chemie Int. Ed.* **2011**, *2*, 10510–10520.
(16) For the utilization of pyridyl-capped clathrochelate complexes as metalloligands see: (a) Jansze, S. M.; Cecot, G.; Wise, M. D.; Zhurov, K. O.; Ronson, T. K.; Castilla, A. M.; Finelli, A.; Pattison, P.; Solari, E.; Scopelliti, R.; Zelinskii, G. E.; Vologzhanina, A. V; Voloshin, Y. Z.; Nitschke, J. R.; Severin, K. *J. Am. Chem. Soc.* **2016**, *138*, 2046-2054; (b) Wise, M. D.; Holstein, J. J.; Pattison, P.; Besnard, C.; Solari, E.; Scopelliti, R.; Bricogne, G.; Severin, K. *Chem. Sci*. **2015**, *6*, 1004–1010; (c) Ardavan, A.; Bowen, A. M.; Fernandez, A.; Fielding, A. J.; Kaminski, D.; Moro, F.; Muryn, C. A.; Wise, M. D.; Ruggi, A.; McInnes, E. J. L.; Severin, K.; Timco, G. A.; Timmel, C. R.; Tuna, F.; Whitehead, G. F. S.; Winpenny, R. E. P. *npj Quantum Inf.* **2015**, *1*, 15012.; (d) Zhang, Y.-Y.; Lin, Y.-J.; Jin, G.-X. *Chem. Commun*. **2014**, *50*, 2327−2329; (e) Wise, M. D.; Ruggi, A.; Pascu, M.; Scopelliti, R.; Severin, K. *Chem. Sci*. **2013**, *4*, 1658–1662.
(17) Khanra, S; Weyhermuller, T.; Bill, E.; Chaudhuri, P. *Inorg. Chem.* **2006**, *45*, 5911–5923.
(18) Pascu, M.; Marmier, M.; Schouwey, C.; Scopelliti, R.; Holstein, J. J.; Bricogne, G.; Severin, K. *Chem. Eur. J.* **2014**, *20*, 5592–5600.
(19) Smithenry, D. W.; Wilson, S. R.; Suslick, K. S. *Inorg. Chem.* **2003**, *42*, 7719–7721.
(20) Kesanli, B.; Cui, Y.; Smith, M. R.; Bittner, E. W.; Bockrath, B. C.; Lin, W. *Angew. Chem. Int. Ed.* **2004**, *44*, 72–75.
(21) Lebed, E. G.; Belov, A. S.; Dolganov, A. V.; Vologzhanina, A. V.; Szebesczyk, A.; Gumienna-Kontecka, E.; Kozlowski, H.; Bubnov, Y. N.; Dubey, I. Y.; Voloshin, Y. Z., *Inorg. Chem. Commun.* **2013,** *30*, 53–57.
(22) Selected examples: (a) Zhang, Y.-Y.; Lin, Y.-J.; Jin, G.-X. *Chem. Commun.* **2014**, *50*, 2327–2329; (b) Wise, M. D.; Ruggi, A.; Pascu, M.; Scopelliti, R.; Severin, K. *Chem. Sci.* **2013**, *4*, 1658-1662 ; (c) Dolganov, A. V; Belov, A. S.; Novikov, V. V; Vologzhanina, A. V; Mokhir, A.; Bubnov, Y. N.; Voloshin, Y. Z. *Dalton Trans.* **2013**, *42*, 4373–4376; (d) Voloshin, Y. Z.; Belaya, I. G.; Belov, A. S.; Platonov, V. E.; Maksimov, A. M.; Vologzhanina, A. V; Starikova, Z. A.; Dolganov, A. V; Novikov, V. V; Bubnov, Y. N. *Dalton Trans.* **2012**, *41*, 737–746; (e) Voloshin, Y. Z.; Varzatskii, O. A.; Belov, A. S.;

Starikova, Z. A.; Strizhakova, N. G.; Dolganov, A. V.; Kochubey, D. I.; Bubnov, Y. N. *Inorg. Chim. Acta* **2010**, *363*, 134–146.
(23) Barder, T. E.; Walker, S. D.; Martinelli, J. R.; Buchwald, S. L. *J. Am. Chem. Soc.,* **2005**, *127*, 4685–4696.
(24) (a) Li, J.; Yang, G.-P.; Wei, S.-L.; Gao, R.-C.; Bai, N.-N.; Wang, Y.-Y. *Cryst. Growth Des.* **2015**, *15*, 5382–5387; (b) Bai, L.; Wang, H.-B.; Li, D.-S.; Wu, Y.-P.; Zhao, J.; Ma, L.-F.; *Inorg. Chem. Commun.* **2014**, *44*, 188–190; (c) Ma, M.-L.; Qin, J.-H.; Ji, C.; Xu, H.; Wang, R.; Li, B.-J.; Zang, S.-Q.; Hou, H.-W.; Batten, S. R. *J. Mater. Chem. C* **2014**, *2*, 1085–1093; (d) Wang, D.; Zhao, T.; Cao, Y.; Yao, S.; Li, G.; Huo, Q.; Liu, Y. *Chem. Commun.* **2014**, *50*, 8648–8650; (e) Duan, X.; Song, R.; Yu, J.; Wang, H.; Cui, Y.; Yang, Y.; Chen, B.; Qian, G. *RSC Adv.* **2014**, *4*, 36419–36424; (f) Schnobrich, J. K.; Lebel, O.; Cychosz, K. A.; Dailly, A.; Wong-Foy, A. G.; Matzger, A. J. *J. Am. Chem. Soc.* **2010**, *132*, 13941–13948.
(25) Selected examples (a) Han, S.; Wei, Y.; Valente, C.; Lagzi, I.; Gassensmith, J. J.; Coskun, A.; Stoddart, J. F.; Grzybowski, B. A. *J. Am. Chem. Soc.* **2010**, *132*, 16358–16361; (b) Horcajada, P.; Chalati, T.; Serre, C.; Gillet, B.; Sebrie, C.; Baati, T.; Eubank, J. F.; Heurtaux, D.; Clayette, P.; Kreuz, C.; Chang, J.-S.; Hwang, Y. K.; Marsaud, V.; Bories, P.-N.; Cynober, L.; Gil, S.; Férey, G.; Couvreur, P.; Gref, R. *Nat. Mater.* **2010**, *9*, 172–178; (c) Lee, J.; Farha, O. K.; Roberts, J.; Scheidt, K. A.; Nguyen, S. T.; Hupp, J. T. *Chem. Soc. Rev.* **2009**, *38*, 1450–9.
(26) Bricogne, G.; Blanc, E.; Brandl, M.; Flensburg, C.; Keller, P.; Paciorek, P.; Roversi, P.; Sharff, A.; Smart, O.; Vonrhein, C.; Womack, T.; BUSTER version 2.13.0, **2011** Global Phasing Ltd., Cambridge, United Kingdom.
(27) http://grade.globalphasing.org
(28) (a) Sheldrick, G. M. Acta Crystallogr. Sect. C Struct. Chem. **2015**, *71*, 3–8; (b) Sheldrick, G. M. *Acta Cryst*. **2008**, *A64*, 112-122.
(29) Thorn, A.; Dittrich, B.; Sheldrick, G. M. *Acta Cryst*. **2012**, *A68*, 448–451.
(30) Hübschle, C. B. ; Sheldrick, G. M.; Dittrich, *J. Appl. Cryst.* **2011**, *44*, 1281–1284
(31) Kratzert, D.; Holstein, J. J.; Krossing, I. *J. Appl. Crystallogr.* **2015**, *48*, 933–938.
(32) Selected examples (a) Tranchemontagne, D. J.; Hunt, J. R.; Yaghi, O. M. *Tetrahedron,* **2008**, *64*, 8553–8557; (b) Rowsell, J. L. C.; Yaghi, O. M. *Microporous Mesoporous Mater.* **2004**, *73*, 3–14.
(33) Selected examples: (a) Jiang, H.-L.; Makal, T. A.; Zhou, H.-C. *Coord. Chem. Rev.* **2013**, *257*, 2232–2249; (b) Zhang, S.-Y.; Zhang, Z.; Zaworotko, M. J. *Chem. Commun.* **2013**, *49*, 9700–9703.
(34) Selected examples: (a) Brozek, C. K.; Bellarosa, L.; Soejima, T.; Clark, T. V.; López, N.; Dincă, M. *Chem. Eur. J.* **2014**, *20*, 6871–6874; (b) Brozek, C. K.; Dincă, M. *Chem. Soc. Rev.* **2014**, *43*, 5456–5467; (c) Brozek, C. K.; Dincă, M. *J. Am. Chem. Soc.* **2013**, *135*, 12886–12891.
(35) Q. Yue, Q. Sun, A.-L. Cheng, E.-Q. Gao, *Cryst. Growth Des.* **2010**, *10*, 44–47
(36) Selected recent examples of MOFs constructed from paddlewheel SBUs: (a) So, M. C.; Beyzavi, M. H.; Sawhney, R.; Shekhah, O.; Eddaoudi, M.; Al-Juaid, S. S.; Hupp, J. T.; Farha, O. K., *Chem. Commun.* **2015**, *51*, 85–88; (b) Hendon, C. H.; Walsh, A., *Chem. Sci.* **2015**, *6*, 3674–3683; (c) Gao, W.-Y.; Cai, R.; Pham, T.; Forrest, K. A.; Hogan, A.; Nugent, P.; Williams, K.; Wojtas, L.; Luebke, R.; Weseliński, Ł. J.; Zaworotko, M. J.; Space, B.; Chen, Y.-S.; Eddaoudi, M.; Shi, X.; Ma, S., *Chem. Mater.* **2015**, *27*, 2144–2151; (d) Kongpatpanich, K.; Horike, S.; Sugimoto, M.; Kitao, S.; Seto, M.; Kitagawa, S., *Chem. Commun.* **2014**, *50*, 2292–2294; (e) Johnson, J. A.; Chen, S.; Reeson, T. C.; Chen, Y.-S.; Zeng, X. C.; Zhang, J., *Chem.-Eur. J.* **2014**, *20*, 7632–7637; (f) Hu, Z.; Tan, K.; Lustig, W. P.; Wang, H.; Zhao, Y.; Zheng, C.; Banerjee, D.; Emge, T. J.; Chabal, Y. J.; Li, J., *Chem. Sci.* **2014**, *5*, 4873–4877; (g) Gong, Q.; Hu, Z.; Deibert, B. J.; Emge, T. J.; Teat, S. J.; Banerjee, D.; Mussman, B.; Rudd, N. D.; Li, J., *J. Am. Chem. Soc.* **2014**, *136*, 16724–16727; (h) Cai, J.; Rao, X.; He, Y.; Yu, J.; Wu, C.; Zhou, W.; Yildirim, T.; Chen, B.; Qian, G., *Chem. Commun.* **2014**, *50*, 1552–1554; (i) Yan, Y.; Yang, S.; Blake, A. J.; Schröder, M., *Acc. Chem. Res.* **2014**, *47*, 296–307; (j) Takaishi, S.; DeMarco, E. J.; Pellin, M. J.; Farha, O. K.; Hupp, J. T., *Chem. Sci.* **2013**, *4*, 1509–1513; (k)

Sakata, Y.; Furukawa, S.; Kondo, M.; Hirai, K.; Horike, N.; Takashima, Y.; Uehara, H.; Louvain, N.; Meilikhov, M.; Tsuruoka, T.; Isoda, S.; Kosaka, W.; Sakata, O.; Kitagawa, S., *Science* **2013**, *339*, 193–196; (l) Peng, Y.; Krungleviciute, V.; Eryazici, I.; Hupp, J. T.; Farha, O. K.; Yildirim, T., *J. Am. Chem. Soc.* **2013**, *135*, 11887–11894; (m) Jin, S.; Son, H.-J.; Farha, O. K.; Wiederrecht, G. P.; Hupp, J. T., *J. Am. Chem. Soc.* **2013,** *135*, 955–958.

(37) Selected examples: (a) Dutta, A.; Koh, K.; Wong-Foy, A. G.; Matzger, A. J. *Angew. Chem. Int. Ed.* **2015***, 54*, 1–6; (b) Liu, L.; Telfer, S. G. *J. Am. Chem. Soc.* **2015**, *137*, 3901–3909; (c) Chae, H. K.; Siberio-Pérez, D. Y.; Kim, J.; Go, Y.; Eddaoudi, M.; Matzger, A. J.; O'Keeffe, M.; Yaghi, O. M. *Nature* **2004**, *427*, 523–527.

(38) Cavka, J. H.; Jakobsen, S.; Olsbye, U.; Guillou, N.; Lamberti, C.; Bordiga, S.; Lillerud, K. P. *J. Am. Chem. Soc.* **2008**, *130*, 13850–13851.

(39) Selected examples: (a) Wang, S.; Wang, J.; Cheng, W.; Yang, X.; Zhang, Z.; Xu, Y.; Liu, H.; Wu, Y.; Fang, M. *Dalton Trans.* **2015**, *44*, 8049–8061; (b) Zhang, M.; Chen, Y.-P.; Bosch, M.; Gentle, T.; Wang, K.; Feng, D.; Wang, Z. U.; Zhou, H.-C. *Angew. Chem. Int. Ed.* **2014**, *53*, 815–818; (c) Jiang, H.-L.; Feng, D.; Wang, K.; Gu, Z.-Y.; Wei, Z.; Chen, Y.-P.; Zhou, H.-C. *J. Am. Chem. Soc.* **2013**, *135*, 13934–13938; (d) Deria, P.; Mondloch, J. E.; Tylianakis, E.; Ghosh, P.; Bury, W.; Snurr, R. Q.; Hupp, J. T.; Farha, O. K. *J. Am. Chem. Soc.* **2013**, *135*, 16801–16804.

(40) Selected examples: (a) Wang, R.; Wang, Z.; Xu, Y.; Dai, F.; Zhang, L.; Sun, D. *Inorg. Chem.* **2014**, *53*, 7086–7088; (b) Jiang, J.; Gándara, F.; Zhang, Y.-B.; Na, K.; Yaghi, O. M.; Klemperer, W. G. *J. Am. Chem. Soc.* **2014**, *136*, 12844–12847; (c) Furukawa, H.; Gándara, F.; Zhang, Y.-B.; Jiang, J.; Queen, W. L.; Hudson, M. R.; Yaghi, O. M. *J. Am. Chem. Soc.* **2014**, *136*, 4369–4381; (d) Feng, D.; Wang, K.; Su, J.; Liu, T.-F.; Park, J.; Wei, Z.; Bosch, M.; Yakovenko, A.; Zou, X.; Zhou, H.-C. *Angew. Chemie Int. Ed.* **2014**, *54*, 149–154.

(41) Selected examples: (a) Wang, K.; Huang, H.; Xue, W.; Liu, D.; Zhao, X.; Xiao, Y.; Li, Z.; Yang, Q.; Wang, L.; Zhong, C. *CrystEngComm.* **2015**, *17*, 3586–3590; (b) Lin, Q.; Bu, X.; Kong, A.; Mao, C.; Zhao, X.; Bu, F.; Feng, P. *J. Am. Chem. Soc*. **2015**, *137*, 2235–2238; (c) DeCoste, J. B.; Peterson, G. W.; Jasuja, H.; Glover, T. G.; Huang, Y.; Walton, K. S. *J. Mater. Chem. A* **2013**, *1*, 5642–5650.

(42) Selected examples: (a) Zheng, J.; Wu, M.; Jiang, F.; Su, W.; Hong, M. *Chem. Sci.* **2015**, *6*, 3466–3470; (b) Beyzavi, M. H.; Klet, R. C.; Tussupbayev, S.; Borycz, J.; Vermeulen, N. A.; Cramer, C. J.; Stoddart, J. F.; Hupp, J. T.; Farha, O. K. *J. Am. Chem. Soc.* **2014**, *136*, 15861–15864. (c) Kim, M.; Cohen, S. M. *CrystEngComm.* **2012**, *14*, 4096–4104; (d) Vermoortele, F.; Ameloot, R.; Vimont, A.; Sebrie, C.; De Vos, D. *Chem. Commun*. **2011**, *47*, 1521–1523.

(43) (a) Mondloch, J. E.; Katz, M. J.; Isley Iii, W. C.; Ghosh, P.; Liao, P.; Bury, W.; Wagner, G. W.; Hall, M. G.; DeCoste, J. B.; Peterson, G. W.; Snurr, R. Q.; Cramer, C. J.; Hupp, J. T.; Farha, O. K. *Nat. Mater.* **2015**, *14*, 512–516; (b) DeCoste, J. B.; Browe, M. A.; Wagner, G. W.; Rossin, J. A.; Peterson, G. W. *Chem. Commun.* **2015**, *51*, 12474–1247; (c) López-Maya, E.; Montoro, C.; Rodríguez-Albelo, L. M.; Aznar Cervantes, S. D.; Lozano-Pérez, A. A.; Cenís, J. L.; Barea, E.; Navarro, J. A. R. *Angew. Chemie Int. Ed.* **2015**, *54*, 6790–6794; (d) Moon, S.-Y.; Liu, Y.; Hupp, J. T.; Farha, O. K. *Angew. Chemie Int. Ed.* **2015**, *54*, 6795–6799; (e) DeCoste, J. B.; Demasky, T. J.; Katz, M. J.; Farha, O. K.; Hupp, J. T. *New J. Chem.* **2015**, *39*, 2396–2399; (f) Decoste, J. B.; Peterson, G. W. *Chem. Rev.* **2014**, *114,* 5695–5727.

(44) Selected examples: (a) Xue, D.-X.; Belmabkhout, Y.; Shekhah, O.; Jiang, H.; Adil, K.; Cairns, A. J.; Eddaoudi, M. *J. Am. Chem. Soc.* **2015**, *137*, 5034–5040; (b) Ren, J.; Langmi, H. W.; North, B. C.; Mathe, M.; Bessarabov, D. *Int. J. Hydrogen Energy* **2014**, *39*, 890–895; (c) Wu, H.; Chua, Y. S.; Krungleviciute, V.; Tyagi, M.; Chen, P.; Yildirim, T.; Zhou, W. *J. Am. Chem. Soc.* **2013**, *135*, 10525–10532; (d) Bon, V.; Senkovskyy, V.; Senkovska, I.; Kaskel, S. *Chem. Commun.* **2012**, *48*, 8407–8409; (a) Schaate, A.; Roy, P.; Godt, A.; Lippke, J.; Waltz, F.; Wiebcke, M.; Behrens, P. *Chem. Eur. J.* **2011**, *17*, 6643–6651; (f) Diring, S.; Furukawa, S.; Takashima, Y.; Tsuruoka, T.; Kitagawa, S. *Chem. Mater*. **2010**, *22*, 4531–4538; (g) Tsuruoka, T.; Furukawa, S.; Takashima, Y.; Yoshida, K.; Isoda, S.; Kitagawa, S. *Angew. Chem. Int. Ed.* **2009**, *48*, 4739–4743; (h) Tsuruoka, T.; Furukawa, S.; Takashima, Y.; Yoshida, K.; Isoda, S.; Kitagawa, S. *Angew. Chem Int. Ed.* **2009**, *121*, 4833–4837.

(45) Representatives examples: (a) Luu, C. L.; Nguyen, T. T. Van; Nguyen, T.; Hoang, T. C. *Adv. Nat. Sci. Nanosci. Nanotechnol.* **2015**, *6*, 025004; (b) Wang, B.; Huang, H.; Lv, X.-L.; Xie, Y.; Li, M.; Li, J.-R. *Inorg. Chem.* **2014**, *53*, 9254–9259. (c) Yang, Q.; Guillerm, V.; Ragon, F.; Wiersum, A. D.; Llewellyn, P. L.; Zhong, C.; Devic, T.; Serre, C.; Maurin, G. *Chem. Commun.* **2012**, *48*, 9831–9833.

(46) Beletskaya, I.; Tyurin, V. S.; Tsivadze, A. Y. ; Guilard, R. ; Stern. C. *Chem. Rev.* **2009**, *109*, 1659–1713.

For table of contents only:

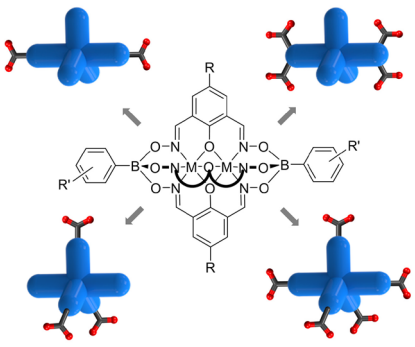

Text for the TOC: Dinuclear clathrochelate complexes can be decorated with two, three, four, or five carboxylic acid groups. The resulting compounds represent interesting metalloligands for supramolecular chemistry and materials science.